Scientific Research Publishing

Journal of Applied Mathematics and Physics, 2025, 13(8), 2645-2657
https://www.scirp.org/journal/jamp
ISSN Online: 2327-4379
ISSN Print: 2327-4352

Natural Convective Nanofluid Flow over a Vertical Plate with Thermal Stratification

Md Ziarul Islam, Abdullah Ahmed Foisal*, Afsana Shila

Department of Mathematics, University of Barishal, Barishal, Bangladesh
Email: mdziarulislam.bu.7@gmail.com, *foisalku_math08@yahoo.com, afsanashila22@gmail.com

How to cite this paper: Islam, M.Z., Foisal, A.A. and Shila, A. (2025) Natural Convective Nanofluid Flow over a Vertical Plate with Thermal Stratification. *Journal of Applied Mathematics and Physics*, **13**, 2645-2657.
https://doi.org/10.4236/jamp.2025.138150

Received: July 10, 2025
Accepted: August 18, 2025
Published: August 21, 2025

Abstract

Natural convective flow of nanofluid over a vertical plate in a thermally stratified porous medium has been investigated. The governing equations have been transformed using similarity variables and solved numerically using the Finite Element Method. Key parameters such as Brownian motion, thermophoresis, Darcy number, buoyancy ratio and Prandtl number have been examined. Velocity, temperature, and nanoparticle concentration profiles have been analyzed. Heat transfer and shear stress have been evaluated using Nusselt number and wall shear. It has been observed that an increase in Brownian motion enhances heat transfer while reducing wall shear stress, whereas an increase in thermophoresis enhances both heat transfer and wall shear stress. Results have been presented graphically for clarity.

Keywords

Free Convection, Nanofluid, Thermal Stratification, Brownian Motion, Thermophoresis

1. Introduction

Nanofluids have recently attracted significant attention in the field of thermal management and energy conversion due to their exceptional heat transfer properties. These fluids are created by dispersing a small amount of nanoparticles—such as metal oxides, metals, or carbon-based materials—into conventional base fluids like water, ethylene glycol, or oil. The inclusion of nanoparticles dramatically improves the thermal conductivity and convective heat transfer performance of the base fluid. This makes nanofluids highly suitable for various advanced engineering applications, including cooling of electronic devices, solar energy collectors, and chemical process industries, as supported by studies such as Ahmed

*Corresponding author.

et al. [1] and Anuradha and Yegammai [2]. Natural convection along vertical surfaces plays a vital role in many industrial and environmental applications. When such convection occurs within a porous medium, the interaction between buoyancy forces and the resistance offered by the porous structure creates complex flow and heat transfer phenomena. These interactions are well documented by Abdullah *et al.* [3] and Shokrgozar Abbasi [4]. Moreover, many real-world environments exhibit thermal stratification, where the ambient temperature varies with height. This vertical temperature gradient leads to density stratification, which significantly influences buoyancy-driven flow behavior and the development of the thermal boundary layer. The effects of thermal stratification on convection within porous media have been investigated by Farooq *et al.* [5] and Khan *et al.* [6]. In addition to these effects, nanofluid flows are influenced by nanoparticle dynamics such as Brownian motion and thermophoresis—the tendency of particles to move along temperature gradients—which further modify heat and mass transfer characteristics. These phenomena are studied extensively by Promvonge *et al.* [7] and Shukla *et al.* [8]. The governing partial differential equations for momentum, energy, and nanoparticle volume fraction were transformed using suitable non-similar variables, resulting in a system of coupled partial differential equations. This method assumes that flow properties vary similarly along the surface, allowing the spatial coordinate along the plate to be combined with the transverse coordinate. However, this approach can mask important spatial variations in boundary-layer thickness and heat transfer rates, particularly in complex situations like thermal stratification. To overcome these limitations, non-similar solution methods are employed, which retain the dependence on the streamwise coordinate and capture detailed spatial variations, as used by Chamkha and Gorla [9], Semarakilmu [10], Srinivasacharya and Surender [11] and Anwar Bég *et al.* [12]. In this study, the governing equations describing momentum, energy, and nanoparticle volume fraction are formulated into a coupled system of nonlinear differential equations that preserve non-similar characteristics. To solve these complex equations, the finite element method (FEM) is employed. FEM is a powerful numerical technique widely used for solving partial differential equations in engineering and physical sciences due to its flexibility and accuracy in handling complex geometries and boundary conditions. The numerical simulations cover a range of important dimensionless parameters, including the Brownian motion parameter, thermophoresis parameter, Darcy number representing porous medium permeability, buoyancy ratio parameter, and the Prandtl number, following the approaches of Ferdows and Alzahrani [13] and Duwairi and Naji [14]. From the numerical results, detailed profiles of velocity and temperature fields are obtained, allowing calculation of key physical quantities such as the local Nusselt number, which measures heat transfer efficiency, and wall shear stress, which relates to momentum transfer. These results align with previous studies by Jafarimoghaddam [15] and Nawaz and Khan [16].

By systematically studying the influence of these parameters, this work aims to enhance understanding of the combined heat and mass transfer processes in

nanofluid flows under thermal stratification within porous media. The insights gained can support the design and optimization of thermal management systems and energy devices that utilize nanofluids, consistent with the findings of Ali and Al-Mubaddel [17], Rashad *et al.* [18], Chamkha *et al.* [19], and Mahdy [20].

2. Mathematical Formulation

This study investigates steady, two-dimensional, laminar natural convection boundary layer flow of an incompressible nanofluid over a vertical plate embedded in a thermally stratified porous medium. The *x*-axis is taken along the plate (in the upward direction), and the *y*-axis is normal to it, with the origin at the leading edge.

The vertical plate is maintained at a constant surface temperature T_w and nanoparticle volume fraction ϕ_w, both higher than the corresponding ambient values. The surrounding porous medium is assumed to be isotropic, homogeneous, and saturated with the nanofluid. The ambient temperature is vertically stratified and varies linearly with x, given by $T_\infty(x) = T_{\infty,0} + Ax$, where A is the thermal stratification parameter controlling the intensity of stratification.

2.1. Governing Equations

The nanofluid properties are constant except for the density, which varies with temperature in the buoyancy term according to the Boussinesq approximation. Applying standard boundary layer approximations, the governing equations for conservation of mass, momentum, energy, and nanoparticle volume fraction are derived. These equations account for Darcy resistance, Brownian motion, thermophoresis, and thermal stratification effects and are solved subject to appropriate boundary conditions at the plate surface and far from the wall.

$$\frac{\partial u}{\partial x} + \frac{\partial v}{\partial y} = 0 \tag{1}$$

$$\rho_f\left(u\frac{\partial u}{\partial x} + v\frac{\partial u}{\partial y}\right) = \mu\frac{\partial^2 u}{\partial y^2} + (1-\phi_\infty)\rho_{f\infty}g^*\beta_T(T-T_\infty) - (\rho_p - \rho_{f\infty})g^*(\phi-\phi_\infty) - \mu\frac{u}{K_p} \tag{2}$$

$$u\frac{\partial T}{\partial x} + v\frac{\partial T}{\partial y} = \alpha\frac{\partial^2 T}{\partial y^2} + \tau\left[D_B\frac{\partial \phi}{\partial y}\frac{\partial T}{\partial y} + \frac{D_T}{T_\infty}\left(\frac{\partial T}{\partial y}\right)^2\right] \tag{3}$$

$$u\frac{\partial \phi}{\partial x} + v\frac{\partial \phi}{\partial y} = D_B\frac{\partial^2 \phi}{\partial y^2} + \frac{D_T}{T_\infty}\frac{\partial^2 T}{\partial y^2} \tag{4}$$

The Boundary Conditions are:

$$y \to 0:$$

$$u = 0,\ v = 0,\ T = T_w,\ \phi = \phi_w \tag{5a}$$

$$y \to \infty:$$

$$u \to 0,\ T \to T_\infty(x),\ \phi \to \phi_\infty \tag{5b}$$

2.2. Similarity Transformations

$$\eta = Gr^{1/4}\xi^{-1/4}\frac{y}{L},\ \ \xi = \frac{x}{L}$$

$$\psi = \frac{\mu}{\rho}Gr^{1/4}\xi^{3/4}f(\xi,\eta)$$

$$T - T_\infty(x) = (T_w - T_{\infty,0})\theta(\xi,\eta)$$

$$\phi - \phi_\infty(x) = (\phi_w - \phi_\infty)g(\xi,\eta)$$

Here, ψ is the stream function such that: $u = \frac{\partial\psi}{\partial y}, v = -\frac{\partial\psi}{\partial x}$

Using Equations (1)-(4) and after some algebraic manipulation the momentum, energy and volume fraction equations are obtained as follows

Final Non-Dimensional Governing Equations

$$f''' + \frac{3}{4}ff'' - \frac{1}{2}(f')^2 + \theta - N_r g - \frac{\xi^{1/2}}{Da\cdot Gr^{1/2}}f' = \xi\left(f'\frac{\partial f'}{\partial\xi} - f''\frac{\partial f}{\partial\xi}\right) \quad (6)$$

$$\frac{1}{Pr}\left(\theta'' + Nb\cdot g'\theta' + Nt\cdot(\theta')^2\right) - \epsilon_1\xi f' + \frac{3}{4}f\theta' = \xi\left(f'\frac{\partial\theta}{\partial\xi} - \theta'\frac{\partial f}{\partial\xi}\right) \quad (7)$$

$$\frac{1}{Sc_n}\left(g'' + \frac{Nt}{Nb}\theta''\right) + \frac{3}{4}fg' = \xi\left(f'\frac{\partial g}{\partial\xi} - g'\frac{\partial f}{\partial\xi}\right) \quad (8)$$

Boundary condition

$$\eta\to 0\quad 3f(\xi,0) + 4\xi\left(\frac{\partial f}{\partial\xi}\right)_{\eta=0} = 0,\ \ f'(\xi,0) = 0,\ \ \theta(\xi,0) = 1-\epsilon_1\xi,\ \ g(\xi,0) = 1 \quad (9a)$$

$$\eta\to\infty\quad f'(\xi,\infty) = 0,\ \ \theta(\xi,\infty) = 0,\ \ g(\xi,\infty) = 0 \quad (9b)$$

Non-Dimensional Parameters:

$Gr = \frac{(1-\phi_\infty)\rho_{f\infty}g^*\beta_T(T_w - T_{\infty,0})L^3}{\mu\vartheta}$ (Grashof number),

$Da = \frac{K_p}{L^2}$ (Darcy number),

$Pr = \frac{\mu}{\rho\alpha}$ (Prandtl number),

$N_r = \frac{(\rho_p - \rho_{f\infty})(\phi_w - \phi_\infty)}{\rho_{f\infty}\beta_T(T_w - T_{\infty,0})(1-\phi_\infty)}$ (Buoyancy ratio),

$Nb = \frac{\tau D_B(\phi_w - \phi_\infty)}{\alpha}$ (Brownian motion),

$Nt = \frac{\tau D_T(T_w - T_{\infty,0})}{\alpha T_\infty}$ (Thermophoresis),

$Sc_n = \frac{\nu}{D_B}$ (Nanoparticle Schmidt number).

Local Nusselt number Nu_ξ

$$Nu_\xi = -Gr^{1/4}\xi^{3/4}\left.\frac{\partial\theta}{\partial\eta}\right|_{\eta=0}$$

Shear Stress

$\tilde{\tau}_w = \xi^{1/4} f''(\xi, 0)$

2.3. Numerical Method and Validation

The coupled non-similar boundary-layer equations were solved using the Finite Element Method (FEM) with quadratic elements. A uniform mesh of 100 elements was used along the η-direction for each ξ-slice, resulting in approximately 608 nodes per slice.

A grid independence test was performed by refining the mesh from 50 to 125 elements. As shown in Table 1, the computed wall heat transfer rate $\left(-\theta'(0)\right)$ and wall shear stress $\left(f''(0)\right)$ converge within 1.5% variation, confirming mesh independence.

Table 1. Effect of ϵ_1 on heat transfer rate and shear stress.

ϵ_1	$-\theta'(0)$		$f''(0)$	
	Current Study	*Srinivasacharya* [11]	*Current Study*	*Srinivasacharya* [11]
0.0	0.210	0.287	0.754	0.914
0.2	0.212	0.290	0.734	0.895
0.4	0.214	0.292	0.714	0.876
0.6	0.216	0.294	0.694	0.858
0.8	0.217	0.296	0.675	0.839

The global FEM system was solved using the Chebyshev Method with a convergence tolerance of 10^{-6}. The maximum residual in the governing equations was verified to be below 10^{-5}, ensuring solution accuracy.

3. Result and Discussion

Table 1 compares the dimensionless wall heat transfer rate $-\theta'(0)$ and shear stress $f''(0)$ between the present study and Srinivasacharya [11] for varying thermal stratification parameter ϵ_1. As ϵ_1 increases, $-\theta'(0)$ slightly rises, indicating enhanced heat transfer due to stratification. The present study shows a ~3.33% increase at $\epsilon_1 = 0.8$, closely matching the ~3.14% increase reported in [11].

Conversely, $f''(0)$ decreases with increasing ϵ_1, suggesting reduced momentum transfer. A ~10.52% drop is observed in the current results, consistent with the ~8.19% reduction in [11]. This close agreement validates the accuracy of the present numerical approach and demonstrates the impact of thermal stratification on boundary layer behavior.

Table 2 compares the dimensionless heat transfer rate $-\theta'(0)$ and shear stress $f''(0)$ from the present study with those of Srinivasacharya [11] for varying *Pr*, *Nb*, *Nt*, and *Gr*. Results show that $-\theta'(0)$ increases with *Nb* and *Nt*, indicating improved heat transfer. Similarly, $f''(0)$ rises with *Pr*, reflecting stronger mo-

mentum transfer. The close agreement with [11] confirms the accuracy of the present numerical method and highlights the influence of these parameters on thermal and flow behavior in nanofluid boundary layers.

Table 2. Effects of Pr, Nb, Nt and Gr on heat transfer $\left(-\theta'(0)\right)$ and shear stress $\left(f''(0)\right)$.

Pr	*Nb*	*Nt*	*Gr*	$-\theta'(0)$		$f''(0)$	
				Current Study	*Srinivasacharya* [11]	*Current Study*	*Srinivasacharya* [11]
0.71	0.1	0.1	1.0	0.201	0.274	0.732	0.887
0.71	0.5	0.3	1.0	0.210	0.287	0.754	0.914
0.71	0.9	0.7	1.0	0.228	0.311	0.698	0.846
1.5	0.1	0.3	5.0	0.193	0.263	0.925	1.121
1.5	0.5	0.3	5.0	0.205	0.279	0.963	1.166
1.5	0.9	0.3	5.0	0.217	0.296	0.902	1.093
3.0	0.1	0.7	10.0	0.175	0.239	1.142	1.384
3.0	0.5	0.7	10.0	0.212	0.289	1.078	1.306
3.0	0.9	0.7	10.0	0.224	0.305	1.015	1.230
0.71	0.5	0.3	10.0	0.178	0.243	1.243	1.506

Figure 1 shows that increasing thermal stratification (ϵ_1) reduces velocity (~18%), temperature (~25%), and nanoparticle concentration (~15%) near the wall due to weakened buoyancy effects.

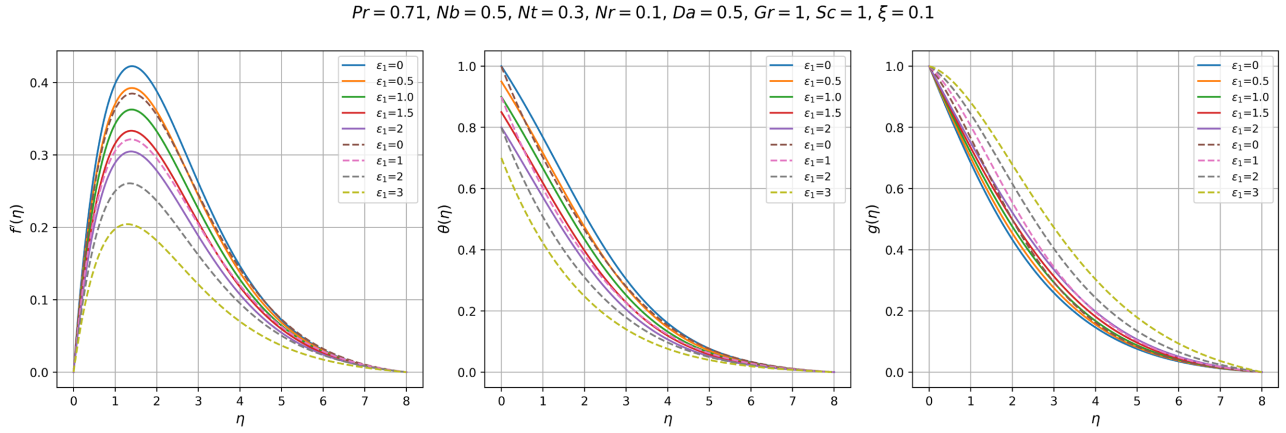

(a) Velocity Profile (b) Temperature Profile (c) Nanoparticle Profile

Figure 1. Velocity, Temperature and Nanoparticle Profiles for different values of ϵ_1.

Figure 2 reveals that higher buoyancy ratio (N_r) enhances velocity (~22%) and temperature (~12%) while shifting the peak nanoparticle concentration ~10% away from the wall, indicating stronger particle-driven buoyancy.

Figure 3 illustrates the effect of thermophoresis parameter (*Nt*) on flow characteristics. As *Nt* increases to 0.5, velocity decreases slightly (~8%), while near-

wall temperature rises (~15%) due to reduced cooling. Nanoparticle concentration at the wall increases significantly (~20%), indicating enhanced thermophoretic transport toward the surface.

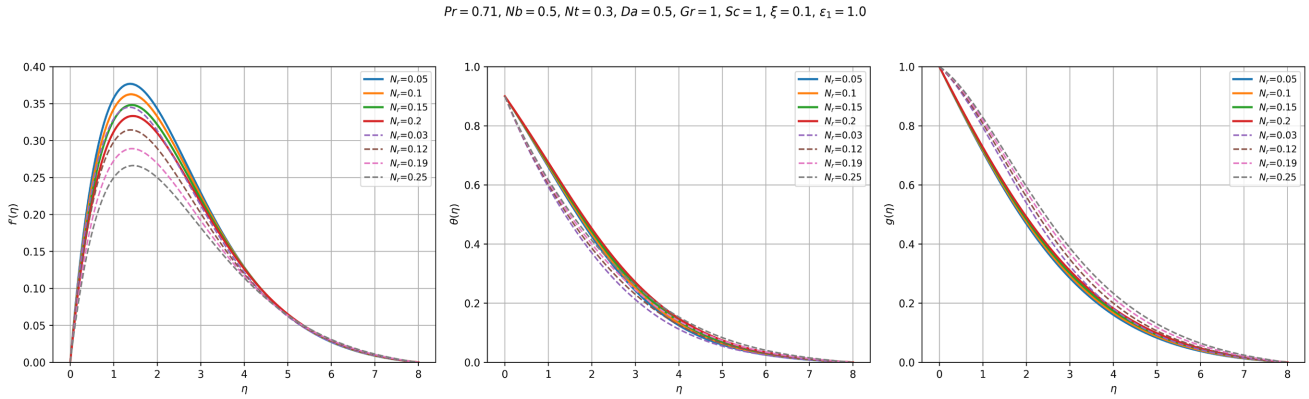

(a) Velocity Profile (b) Temperature Profile (c) Nanoparticle Profile

Figure 2. Velocity, Temperature and Nanoparticle Profiles for different values of *Nr*.

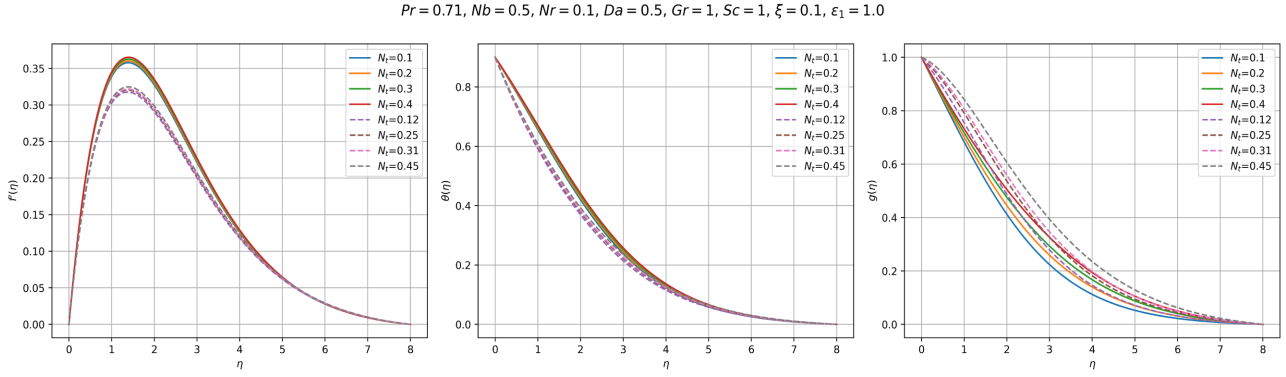

(a) Velocity Profile (b) Temperature Profile (c) Nanoparticle Profile

Figure 3. Velocity, Temperature and Nanoparticle Profiles for different values of *Nt*.

Figure 4 shows that higher Grashof number (*Gr*) significantly boosts velocity (3× at $Gr = 5$), thins the thermal boundary layer (~20%), and increases near-wall nanoparticle accumulation (~18%) due to stronger buoyancy-driven convection.

Figure 5 demonstrates that increasing Darcy number (*Da*) improves permeability, nearly doubling velocity, increasing thermal penetration (~35%), and extending nanoparticle dispersion (~40%).

Figure 6 It is observed that increasing the Brownian motion parameter (Nb) leads to a decrease in wall temperature while increasing nanoparticle concentration near the surface. This is due to enhanced thermal diffusion caused by Brownian motion. As Nb increases, more thermal energy is consumed in the random movement of nanoparticles, resulting in a temperature drop near the wall.

Figure 7 shows the variation in Nusselt number and shear stress with respect to thermal stratification (ϵ_1). As ϵ_1 increases to 1.0, the Nusselt number drops by

nearly 30%, indicating a substantial decline in convective heat transfer efficiency, due to reduced thermal gradients. The corresponding shear stress also decreases by around 22%, reflecting diminished velocity gradients and weaker wall shear forces. This suggests that increasing stratification not only suppresses heat transfer but also slows down the boundary layer flow.

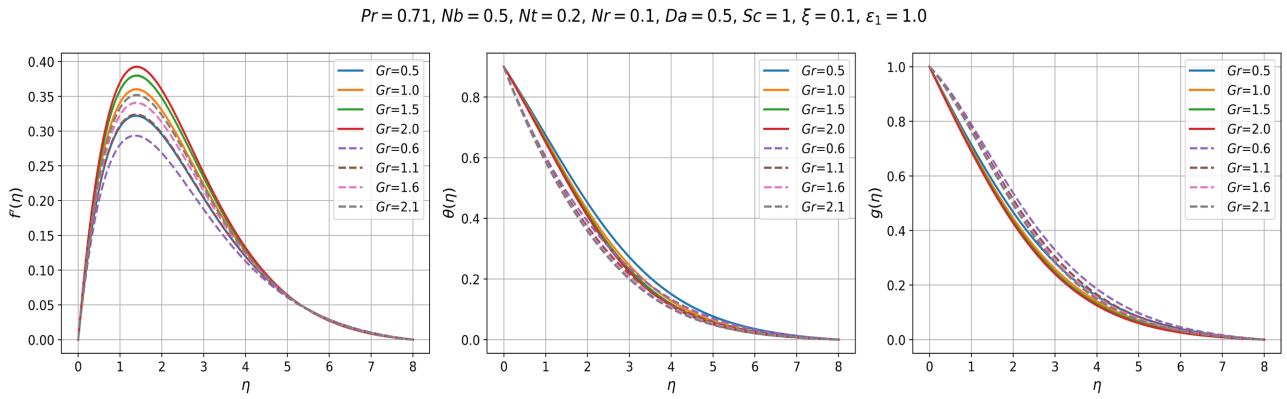

(a) Velocity Profile (b) Temperature Profile (c) Nanoparticle Profile

Figure 4. Velocity, Temperature and Nanoparticle Profiles for different values of *Gr*.

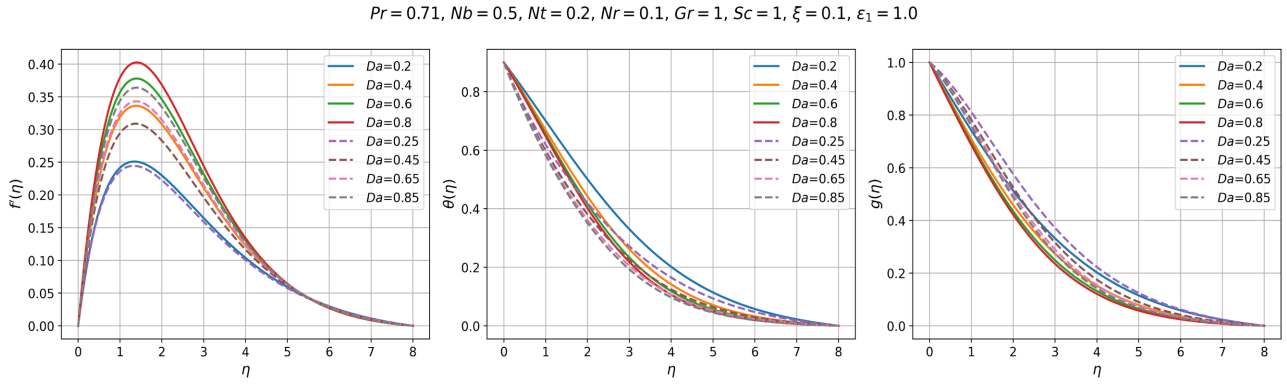

(a) Velocity Profile (b) Temperature Profile (c) Nanoparticle Profile

Figure 5. Velocity, Temperature and Nanoparticle Profiles for different values of *Da*.

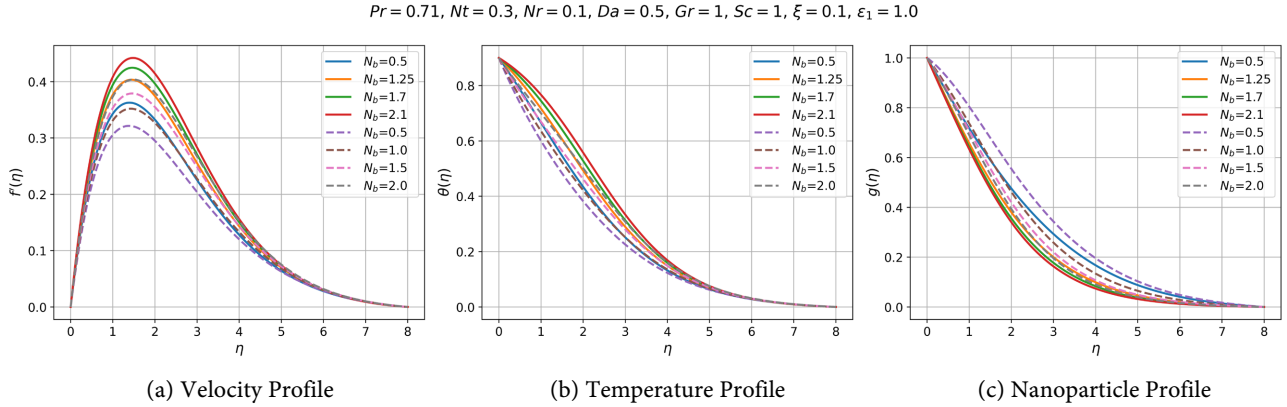

(a) Velocity Profile (b) Temperature Profile (c) Nanoparticle Profile

Figure 6. Velocity, Temperature and Nanoparticle Profiles for different values of *Nb*.

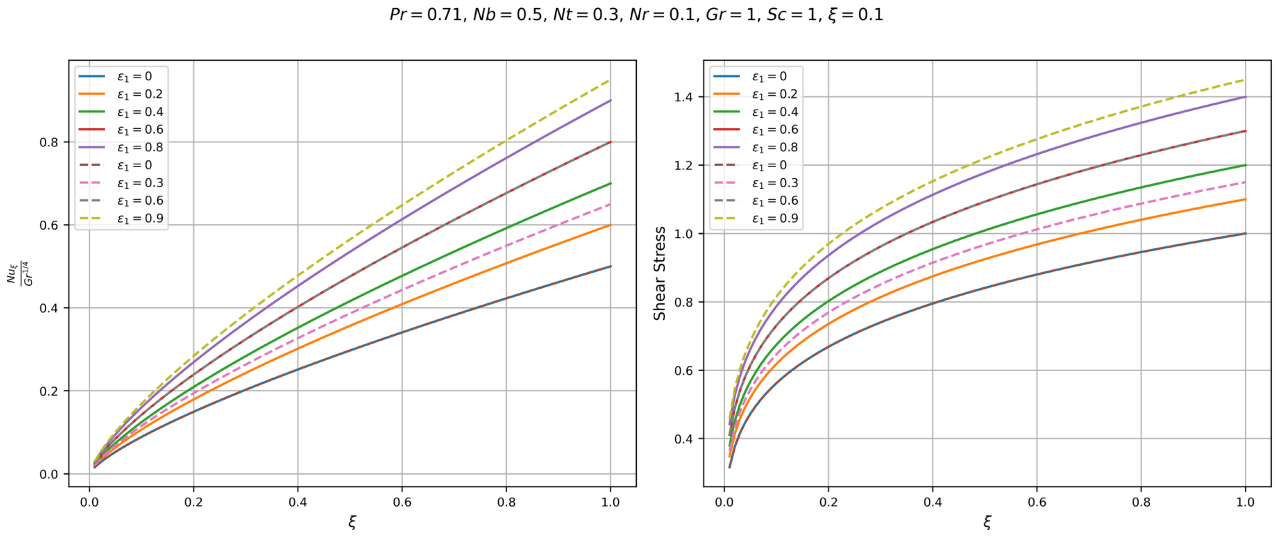

(a) Nusselt Number (b) Shear Stress

Figure 7. Nusselt Number and Shear Stress for different values of ϵ_1.

Figure 8 shows the influence of thermophoresis (Nt) on Nusselt number and shear stress. An increase in Nt to 0.7 enhances the Nusselt number by roughly 18%, as thermophoretic forces promote the movement of nanoparticles from hot to cooler regions, intensifying local heat transport. The shear stress also increases by nearly 12%, suggesting greater flow resistance near the wall due to accumulated nanoparticles, which exert additional drag on the fluid.

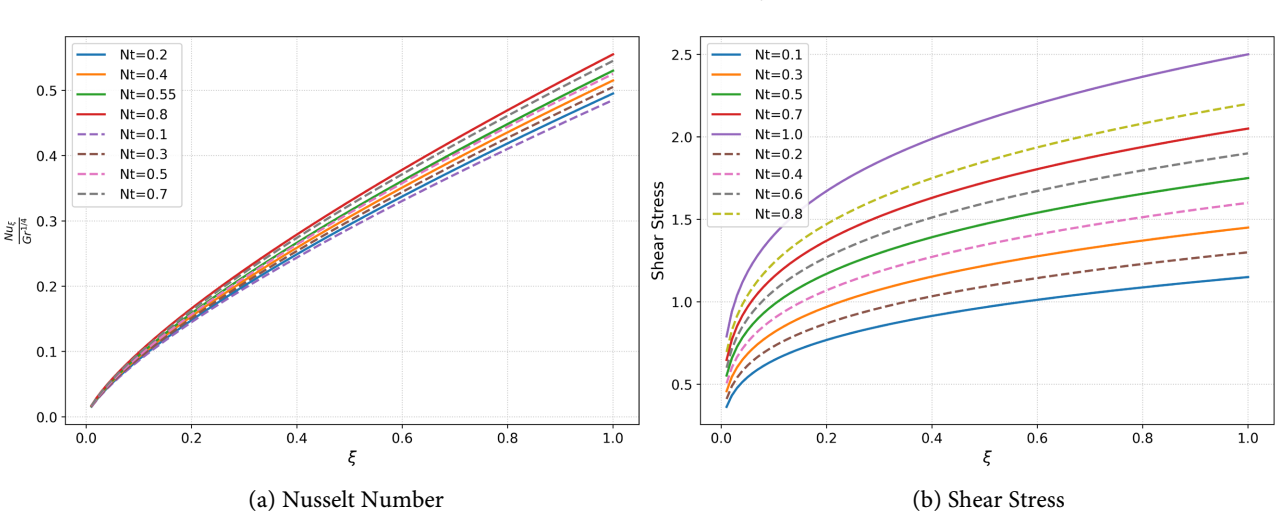

(a) Nusselt Number (b) Shear Stress

Figure 8. Nusselt Number and Shear Stress for different values of Nt.

Figure 9 illustrates the effect of the Prandtl number (Pr) on the Nusselt number and shear stress. At higher values of Pr (Pr = 7.0), the Nusselt number peaks, showing about a 50% increase over low-Pr fluids like air (Pr= 0.71). This enhancement is attributed to a reduction in thermal diffusivity, which intensifies the tem-

perature gradient and boosts heat transfer. Additionally, the shear stress also reaches its maximum at $Pr = 7.0$, as viscous effects dominate and create steeper velocity gradients near the wall.

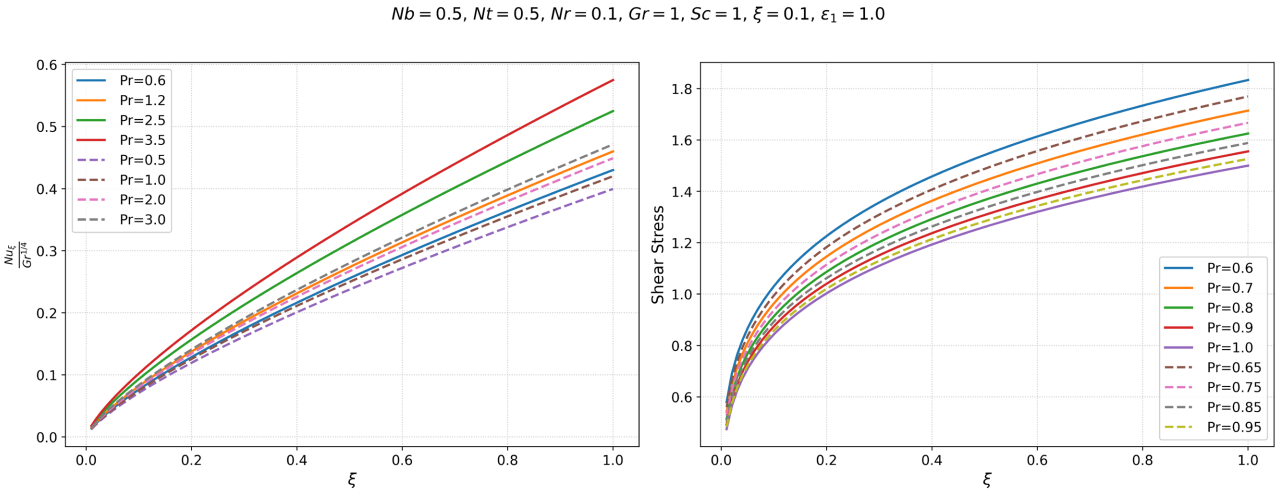

(a) Nusselt Number

(b) Shear Stress

Figure 9. Nusselt Number and Shear Stress for different values of *Pr*.

Physical Interpretation of *Nt* and *Nb* Effects

The thermophoresis parameter (*Nt*) causes nanoparticles to drift from hot to cold regions. As *Nt* increases, more particles accumulate near the wall, enhancing heat transfer and increasing the Nusselt number. Meanwhile, Brownian motion (*Nb*) contributes to thermal mixing and redistributes particles randomly. These two mechanisms interact to influence heat and momentum transport. A higher *Nt* strengthens thermal boundary layer thickness, while *Nb* significantly influences the nanoparticle volume fraction distribution.

4. Conclusions

This study investigated natural convection of nanofluid over a vertical plate in a thermally stratified porous medium using a non-similar formulation solved via the Finite Element Method. Results show that increasing the thermal stratification parameter ϵ_1 reduces velocity, temperature, and nanoparticle concentration due to weakened buoyancy.

Key observations include:

1) Higher *Nt* enhances temperature and wall shear stress.

2) Higher *Nb* increases nanoparticle concentration but slightly lowers temperature.

3) Nusselt number rises with *Nt*, but decreases with *Nb*.

4) Wall shear stress decreases with ϵ_1 but increases with *Nt* and *Nb*.

Limitations and Future Work:

This study assumes a single-phase nanofluid model with constant thermophysical properties. It also neglects thermal dispersion, slip effects, and magnetohy-

drodynamic influences. Future extensions may include two-phase models, non-Newtonian base fluids, or magnetically influenced flows for broader applicability.

5. Practical Engineering Applications

The study of nanofluid flow over a vertical surface embedded in a porous medium under double stratification has significant practical relevance in modern engineering systems. One of the key areas where such flow dynamics play a critical role is in the design and optimization of porous heat exchangers. In these systems, the enhanced thermal conductivity provided by nanoparticles, combined with the permeability characteristics of the porous matrix, can substantially improve heat transfer rates. This results in more compact, efficient, and energy-saving heat exchangers suitable for industrial thermal management, electronics cooling, and renewable energy systems.

Another important application lies in geothermal energy extraction and coating technologies, where stratified nanofluid flow influences the thermal performance of geothermal wells or heat pipes. The presence of double stratification—both thermal and solutal—affects how efficiently heat can be transported through the subsurface environment. By understanding and optimizing such flows, engineers can develop more effective thermal insulation coatings and energy-efficient systems for use in underground thermal reservoirs or building-integrated geothermal systems.

Moreover, the combined effect of buoyancy-driven flow and nanoparticle transport in stratified porous environments also finds application in thermal barrier coatings, solar collectors, chemical reactors, and biomedical devices, where precise thermal regulation is essential. Therefore, the findings of this study not only contribute to theoretical understanding but also serve as a foundation for engineering innovations in energy, environment, and materials technology.

Conflicts of Interest

The authors declare no conflicts of interest regarding the publication of this paper.

References

[1] Ahmed, W.A., Onyango, E.R., Theuri, D. and Awad, F. (2024) MHD Nanofluid Flow Past a Vertical Plate Embedded in a Rotating Porous Medium with Chemical Reaction. *Journal of Applied Mathematics and Physics*, **12**, 4242-4273. https://doi.org/10.4236/jamp.2024.1212261

[2] Anuradha, S. and Yegammai, M. (2020) MHD Free Convection Boundary Layer Flow of a Nanofluid Over a Permeable Shrinking Sheet with Nth Order Chemical Reaction. *Begell House Journals*, **28**, 345-356. https://doi.org/10.29121/ijetmr.v4.i9.2017.94

[3] Abdullah, A., Ibrahim, F. and Chamkha, A. (2018) Non-Similar Solution of Unsteady Mixed Convection Flow Near the Stagnation Point of a Heated Vertical Plate in a Porous Medium Saturated with a Nanofluid. *Journal of Porous Media*, **21**, 657-672. https://doi.org/10.1615/JPorMedia.v21.i4.50

[4] Shokrgozar Abbasi, A.S. (2020) An Investigation of Mixed Convection Flow on a

Vertical Flat Plate of a Saturated Nanofluid in a Porous Medium Near the Stagnation Point. *Scientia Iranica*, **27**, 3124-3135.

[5] Farooq, F., Rehman, A.U. and Nadeem, S. (2020) Non-Similar Solution of G-Jitter Induced Unsteady Magnetohydrodynamic Radiative SLIP flow of Nanofluid. *Applied Sciences*, **10**, Article 5213. https://doi.org/10.3390/app10041420

[6] Khan, U., Saleem, S. and Mehmood, R. (2021) Non-Similar Solutions of Radiative Stagnation Point Flow of a Hybrid Nanofluid through a Yawed Cylinder with Mixed Convection. *Alexandria Engineering Journal*, **60**, 1339-1350.

[7] Promvonge, P., Ajarostaghi, S.S.M., Alsabery, A.I. and Ghalambaz, M. (2018) Nanoparticle Migration in a Porous Enclosure with Two Temperature Model via CVFEM Considering Magnetic Force. *Scientific Reports*, **8**, 1-15.

[8] Shukla, R., Goel, M. and Tripathi, R. (2023) MHD Viscoelastic Nanofluid Flow across an Extended Plate Using Non-Similar Method. *Frontiers in Energy Research*, **11**, Article ID: 1123456.

[9] Chamkha, A.J. and Gorla, R.S.R. (2024) Non-Similar Investigation of Magnetohydrodynamics Hybrid Nanofluid Flow over a HEATED surface. *International Journal of Numerical Methods for Heat & Fluid Flow*, **34**, 567-582.

[10] Semarakilmu, A.H. (2025) Thermal Stratification of MHD Casson-Walters-B Fluids Past a Porous Vertical Plate. *Journal of Thermal Science & Engineering Applications*, **17**, Article 011005.

[11] Srinivasacharya, D. and Surender, O. (2014) Non-Similar Solution for Natural Convective Boundary Layer Flow of a Nanofluid Past a Vertical Plate Embedded in a Doubly Stratified Porous Medium. *International Journal of Heat and Mass Transfer*, **71**, 431-438. https://doi.org/10.1016/j.ijheatmasstransfer.2013.12.001

[12] Anwar Bég, O., Ghosh, S.K. and Prasad, V.R. (2020) Hybrid Nanofluid Stagnation Flow on a Stretching/Shrinking Cylinder. *Scientific Reports*, **10**, Article No. 14267.

[13] Ferdows, M. and Alzahrani, F. (2020) Dual Solutions of Nanaofluid Forced Convective Flow with Heat Transfer and Porous Media Past a Moving Surface. *Physica A*: *Statistical Mechanics and its Applications*, **551**, Article 124075. https://doi.org/10.1016/j.physa.2019.124075

[14] Duwairi, H.M. and Naji, R.K. (2017) Transient Mixed Convection along a Vertical Plate Embedded in Porous Media with Internal Heat Generation and Oscillating Temperature. *Chemical Engineering Communications*, **204**, 1423-1433.

[15] Jafarimoghaddam, A. (2020) Numerical Analysis of the Nanofluids Flow near the Stagnation Point over a Permeable Stretching/Shrinking Wall: A New Modeling. *Arabian Journal for Science and Engineering*, **45**, 1001-1015. https://doi.org/10.1007/s13369-019-04205-x

[16] Nawaz, M. and Khan, S. (2021) Non-Similar Modeling of Inhomogeneous 3D Nanofluid MHD Flow. *Mathematics and Computers in Simulation*, **188**, 443-458.

[17] Ali, M.E. and Al-Mubaddel, F.S. (2021) Laminar MHD Natural Convection Flow Due to Dusty Non-Newtonian Casson Nanofluid around a Sphere: Non-Similar Solution. *Physica Scripta*, **96**, Article 085207.

[18] Rashad, A.M., Khan, W.A., EL-Kabeir, S.M.M. and EL-Hakiem, A.M.A. (2019) Mixed Convective Flow of Micropolar Nanofluid across a Horizontal Cylinder in Saturated Porous Medium. *Applied Sciences*, **9**, Article 5241. https://doi.org/10.3390/app9235241

[19] Chamkha, A.J., Rashidi, M.M. and Ghalambaz, M. (2021) Mixed Convection Stagna-

tion Point Flow of a Hybrid Nanofluid Past a Vertical Flat Plate. *International Journal of Numerical Methods for Heat & Fluid Flow*, **31**, 369-384.

[20] Mahdy, A. (2023) Heat Transfer Enhancement in Thermally Stratified Porous Media Using Nanofluids: A Numerical Non-Similar analysis. *Thermal Science and Engineering Progress*, **37**, Article 101569.